Isotopic evidence for quasi-equilibrium chemistry in thermally mature natural gases

Nivedita Thiagarajan[a,1], Hao Xie[a], Camilo Ponton[b], Nami Kitchen[a], Brian Peterson[c], Michael Lawson[d], Michael Formolo[e], Yitian Xiao[e], and John Eiler[a]

[a]Department of Geological and Planetary Sciences, California Institute of Technology, Pasadena, CA 91125; [b]Geology Department, Western Washington University, Bellingham, WA 98225; [c]ExxonMobil Corporate Strategic Research, Annandale, NJ 08801; [d]ExxonMobil Upstream Business Development, Spring, TX 77389; and [e]ExxonMobil Upstream Research Company, Spring, TX 77389

Edited by Mark H. Thiemens, University of California San Diego, La Jolla, CA, and approved January 17, 2020 (received for review April 25, 2019)

Natural gas is a key energy resource, and understanding how it forms is important for predicting where it forms in economically important volumes. However, the origin of dry thermogenic natural gas is one of the most controversial topics in petroleum geochemistry, with several differing hypotheses proposed, including kinetic processes (such as thermal cleavage, phase partitioning during migration, and demethylation of aromatic rings) and equilibrium processes (such as transition metal catalysis). The dominant paradigm is that it is a product of kinetically controlled cracking of long-chain hydrocarbons. Here we show that C_{2+} *n*-alkane gases (ethane, propane, butane, and pentane) are initially produced by irreversible cracking chemistry, but, as thermal maturity increases, the isotopic distribution of these species approaches thermodynamic equilibrium, either at the conditions of gas formation or during reservoir storage, becoming indistinguishable from equilibrium in the most thermally mature gases. We also find that the pair of CO_2 and C_1 (methane) exhibit a separate pattern of mutual isotopic equilibrium (generally at reservoir conditions), suggesting that they form a second, quasi-equilibrated population, separate from the C_2 to C_5 compounds. This conclusion implies that new approaches should be taken to predicting the compositions of natural gases as functions of time, temperature, and source substrate. Additionally, an isotopically equilibrated state can serve as a reference frame for recognizing many secondary processes that may modify natural gases after their formation, such as biodegradation.

stable isotopes | compound-specific isotope analysis | clumped isotopes | natural gas | methane

Natural gas is primarily composed of volatile alkanes containing five or fewer carbon atoms and is widely distributed in the subsurface. It is a key resource (1), and is increasingly viewed as a transition fuel that can reduce CO_2 emissions relative to coal and oil as the world's economies move toward carbon-free energy systems. However, the utilization of natural gas poses environmental risks, as leakage contributes significantly to total atmospheric methane, a significant greenhouse gas. Ethane, propane, and butane have short atmospheric lifespans, but they also increase the production of tropospheric ozone, a respiratory hazard and pollutant (2, 3).

Understanding the mechanisms of natural gas formation is critical for predicting where it forms in economic volumes and for recognizing its release to the environment. Hydrocarbons in natural gas are believed to come from two sources, one from biological processes ("biogenic gas") (4) and the other from the thermal cracking of kerogen and oil ("thermogenic gas"). There is disagreement over the origin of thermogenic gas. The predominant view is that it is created by irreversible, thermally activated breakdown of hydrocarbon solids and liquids, with reactions dominated by the cleavage of carbon–carbon bonds (or "cracking") (5, 6) (Fig. 1*A*). However, laboratory experiments involving heating of hydrocarbons generally produce hydrocarbon gases that differ in molecular composition from natural gases. Natural gas reservoirs tend to have greater than 80% methane, while pyrolysis experiments only produce 10 to 65% methane (7–10). Additionally hydrocarbons exist in geologic environments at temperatures that are much greater than their predicted stability based on experimentally derived models of catagenesis (11, 12).

Most explanations for this discrepancy argue that natural gas is generated with a chemistry more similar to products of cracking experiments, but its molecular proportions are then modified by secondary processes, such as methane enrichment by buoyancy-driven fractionation during the migration of gas from its source reservoir (13, 14) or methane enrichment from exceptionally high-temperature catagenesis at equivalent thermal maturities far in excess of those explored by most experiments (12). Additionally, methane-rich thermogenic gases are often suspected of containing a component of biogenic gas (e.g., ref. 15). None of these processes challenge the fundamental view of catagenesis as a family of irreversible reactions that break down larger hydrocarbon molecules to form smaller ones (Fig. 1*A*).

One alternative hypothesis holds that thermogenic gases are generated through catalytic equilibrium processes. Previous work has suggested that hydrocarbons, water, and authigenic minerals in hydrocarbon reservoirs are in a metastable equilibrium (16–19), while other laboratory experiments have suggested that methane, ethane, and propane are in a metathetic equilibrium (20). Support for the metastable equilibrium hypothesis comes from theoretical calculations (16) as well as laboratory experiments that mix precursor hydrocarbons with catalysts, which, upon heating, produce low-molecular weight *n*-alkane gases with molecular proportions

Significance

The mechanisms of natural gas formation are important to the carbon cycle and predicting where economical amounts of natural gas form. However, the formation mechanisms of natural gas are not clear, with hypotheses including both irreversible chemical processes such as thermal cracking of long-chain hydrocarbons and thermodynamic equilibrium processes such as transition metal catalysis. Here we show that hydrocarbon species in natural gases are initially produced by irreversible cracking chemistry, but, as thermal maturity increases, the H and C isotopic distributions within and among coexisting light *n*-alkanes approach thermodynamic equilibrium, either at the conditions of gas formation or during reservoir storage. Our finding has significant implications for natural gas exploration.

Author contributions: N.T., H.X., C.P., and J.E. designed research; N.T., H.X., C.P., N.K., B.P., M.L., M.F., and Y.X. performed research; N.T., H.X., C.P., and J.E. analyzed data; and N.T., H.X., C.P., B.P., M.L., M.F., and J.E. wrote the paper.

The authors declare no competing interest.

This article is a PNAS Direct Submission.

[1]To whom correspondence may be addressed. Email: nivedita@caltech.edu.

This article contains supporting information online at https://www.pnas.org/lookup/suppl/doi:10.1073/pnas.1906507117/-/DCSupplemental.

First published February 11, 2020.

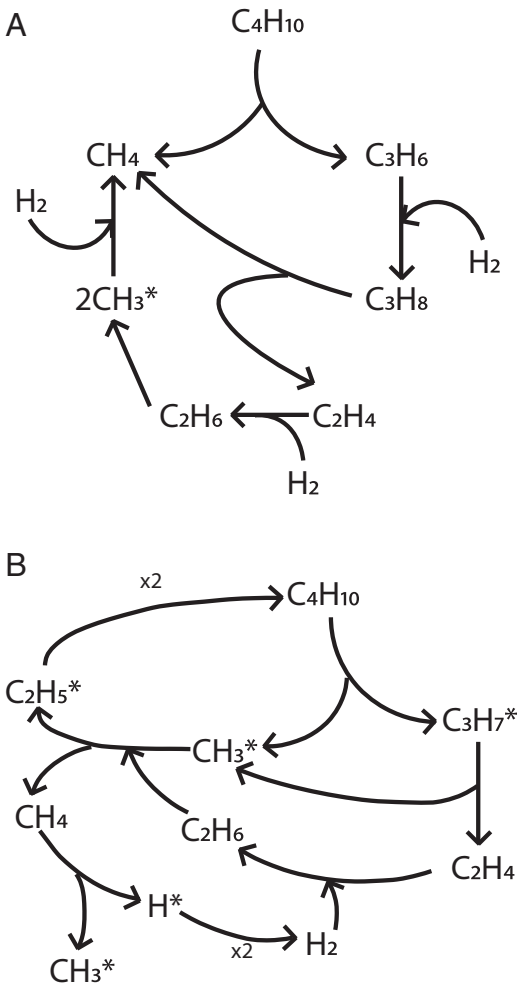

Fig. 1. (*A*) A schematic showing examples of butane degradation through irreversible cracking reactions, and (*B*) a reversible radical reaction network. *, radical.

more closely resembling natural gases (21–23). Finally, another hypothesis is that thermogenic gases are created by a network of radical chain reactions among the gas species, dominated by fast radical transfer reactions and beta-scission leading to thermodynamic equilibrium (Fig. 1*B*). If these equilibrium hypotheses are correct, it implies that natural gases are products of thermal breakdown of larger hydrocarbons, but form gases in proportions governed by the free energies of formation of alkanes and related alkenes and radicals, rather than the rate constants for irreversible cracking of large molecules. This difference would substantially change how we predict and interpret the chemistry of natural gases as functions of temperature, time, and compositions of source substrates.

The distributions of naturally occurring stable isotopes (principally ^{13}C and D) within and between the molecular constituents of natural gases offer tests of whether thermogenic gas production is controlled by irreversible cracking or equilibrium processes. Cracking chemistry yields products having isotopic contents that depend on the compositions of the substrates and the kinetic isotope effects (KIEs) associated with irreversible reactions, whereas systems in a metastable equilibrium have isotopic distributions closely resembling thermodynamic equilibrium, which can be predicted based on the partition function ratios of the compounds of interest. It has been previously shown that methane, ethane, and propane in some natural gases have molecular proportions and $^{13}C/^{12}C$ ratios that resemble thermodynamic equilibrium and not thermal cleavage (21).

Here we extend that argument in three ways: 1) We have measured or compiled C and H isotopic compositions of methane (C_1), ethane (C_2), propane (C_3), butane (C_4), pentane (C_5), and CO_2 for 119 gases from 20 conventional, unconventional, oil-associated, and nonassociated natural deposits around the world. This extended database provides a far wider sampling and allows us to use stricter tests of the equilibrium hypothesis than have been previously considered. 2) Additionally, we include methane clumped isotope compositions (Δ_{18} values) for a large subset of the gases we examine (24–26). The Δ_{18} value principally reflects enrichment (or depletion) in $^{13}CH_3D$ relative to a stochastic distribution of ^{13}C and D among all methane isotopologues, and, in isotopically equilibrated systems, the Δ_{18} value is a function of temperature. 3) We compare measured isotopic compositions to a comprehensive set of theoretically predicted equilibrium and nonequilibrium fractionations between CO_2 and C_1 to C_5 species. Our equilibrium models are based on new ab initio calculations of molecular partition function ratios (see *SI Appendix* for details). Models of nonequilibrium carbon and hydrogen isotope fractionations are based on previous estimates of KIEs associated with homolytic cleavage and beta-scission of methyl, ethyl, propyl, butyl, and pentyl radicals from an *n*-alkane precursor (27, 28) (*SI Appendix*).

Results and Discussion

We find that our most thermally immature samples ($R_o < 0.8$) are consistent with stable isotope distributions controlled by KIEs. However, natural gases of moderate or greater maturity ($R_o > 0.8$) have C_{2+} gases (ethane, propane, butane, and pentane) that are consistent with thermodynamic equilibrium for carbon (Fig. 2 and *SI Appendix*, Fig. S1) and hydrogen isotopes (*SI Appendix*, Fig. S2), considering the combined analytical and model uncertainties. This pattern is also seen in a global compilation (29) of natural gases (*SI Appendix*, Fig. S3). There are three important exceptions to this pattern which we discuss in the following paragraphs.

One subset of gases that are significant exceptions to this generalization have $\varepsilon^{13}C$ (C_3-C_2) values greater than 5‰ and do not fall on or near the thermodynamic equilibrium fractionation line in Fig. 2. These samples are shaded in Fig. 2 and *SI Appendix*, Fig. S2 and share several other traits: All have low apparent Δ_{18} temperatures and relatively low $\delta^{13}C$ and δD of CH_4, and tend to have higher than average values for $\delta^{13}C$ of CO_2. These isotope signatures are all suggestive of biodegradation of oil and/or gas and resemble isotopic signatures previously seen in natural gases from the Antrim Shale, Michigan—a biodegraded natural gas deposit (30, 31).

Another subset of gases that are not in isotopic equilibrium are the hydrogen isotopes of *i*-butane and *i*-pentane (*SI Appendix*, Fig. S4). This deviation could be an analytical artifact, as it is difficult to separate *i*-alkanes from *n*-alkanes. Another possibility is that these species are actually not in equilibrium, and branched *i*-alkanes do not form in the same manner that *n*-alkanes do.

Third, we observe that methane and CO_2 generally are not coequilibrated with the C_2 to C_5 hydrocarbons in natural gases from most basins (*SI Appendix*, Fig. S5). Instead, we find that this pair of compounds exhibits its own pattern of isotopic signatures that suggest a second quasi-equilibrated population, separate from the C_2 to C_5 compounds. This feature is best illustrated in a plot of $\varepsilon^{13}C$ (CO_2–CH_4) vs. the methane clumped isotope apparent temperature, which shows that 73% of gas samples having $C_1/(C_2+C_3) < 20$ (in the thermogenic range) are consistent with mutual thermodynamic equilibrium for the methane Δ_{18} value and the intermolecular equilibrium for $^{13}C/^{12}C$ exchange between CO_2 and CH_4 (Fig. 3). It has been previously suggested that transition metal catalysts can facilitate carbon isotope equilibrium between CO_2 and CH_4 (18). A notable exception to this trend is the suite of

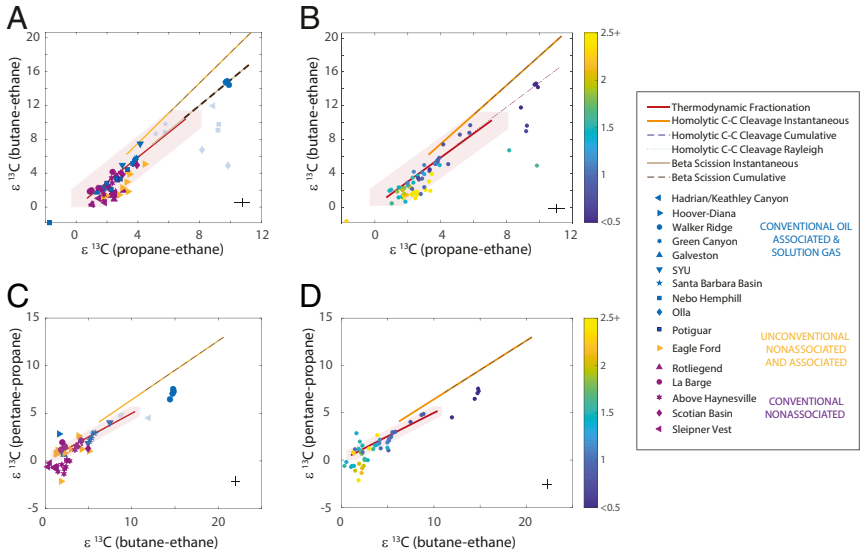

Fig. 2. $\varepsilon^{13}C$ (butane–ethane) vs. $\varepsilon^{13}C$ (propane–ethane), and $\varepsilon^{13}C$ (pentane–propane) vs. $\varepsilon^{13}C$ (propane–ethane), color-coded by (*A* and *C*) reservoir name or (*B* and *D*) R_o, a proxy for thermal maturity calculated via $\delta^{13}C$ of ethane (46). Eighty-eight percent of measured carbon isotopes of C_2-C_4 species and 68% of pentane species are consistent with being in thermodynamic equilibrium. Hydrocarbons initially form through homolytic cleavage (yellow and blue lines) or β-scission (brown lines) mechanisms, as seen in the most-immature reservoirs in our datasets, such as Walker Ridge and Keathley Canyon. As maturity (time and temperature) increases, a radical reaction network chemistry or catalytic chemistry begins to operate, and the reservoirs approach isotopic equilibrium. The approach to equilibrium is seen in moderate-maturity reservoirs such as Green Canyon and SYU. The reservoirs that are the most mature, such as Sleipner Vest, Galveston, Above Haynesville, and Hogsback, show compositions characteristic of having reached isotopic equilibrium (red solid line). The shaded gases are gases associated with biodegradation.

Eagle Ford gases, which have $\varepsilon^{13}C$ (CO_2–CH_4) values of 40 to 46‰, consistent with equilibration at temperatures of 100 °C to 140 °C—similar to the reservoir temperature of ∼140 °C—but methane clumped isotope compositions suggesting apparent temperatures of ≥200 °C, and, in some cases, exceeding the nominal upper bound of thermogenic gas generation of 250 °C (24, 26, 32). Several hypotheses have been put forward to explain the high apparent methane clumped isotope temperatures of Eagle Ford gases, including analytical artifacts and KIEs related to secondary cracking (30). Thus, the deviation of Eagle Ford gases from this pattern of CH_4–CO_2 equilibrium may reflect the fact that they are an unusual case where thermogenic methane clumped isotope apparent temperatures do not approach methane formation temperatures (26).

Some gas samples with $C_1/(C_2+C_3) > 20$—generally considered indicative of biogenic gas or supermature thermogenic gas—show $\varepsilon^{13}C$ (CO_2–C_1) fractionations greater than, equal to, and less than equilibrium values at the temperatures corresponding to methane Δ_{18} value (Fig. 3). The Santa Barbara Basin seep samples have an $\varepsilon^{13}C$ (CO_2–C_1) much greater than expected for equilibrium values, reflecting unusually high $\delta^{13}C$ of CO_2 (∼22‰) with moderate $\delta^{13}C$ of CH_4 (∼ −40‰) and elevated [CO_2]. We suggest that the high $\delta^{13}C$ of CO_2 values as well as the large $\varepsilon^{13}C$ (CO_2–C_1) (which corresponds to a temperature of ∼10 °C) in this suite is due to methanotrophic processes increasing CO_2 concentrations and driving CO_2 and C_1 to equilibrate, possibly associated with sulfate-dependent methane oxidation in shallow sediments at bottom-water temperatures. A second noteworthy exception of this kind is the coal-derived gases in the Rotliegend field, which have $\varepsilon^{13}C$ (CO_2–C_1) values much lower than values predicted for thermodynamic equilibrium and have the highest $\delta^{13}C$ of CH_4 values of the suite. These coal-derived gas samples (33) could have a different set of precursors than the gases derived from marine source rocks, which are the bulk of the rest of the suite. The high-maturity Haynesville Shale formation in addition to the biodegraded gases (Nebo Hemphill and Olla) have C_1/C_{2+3} ratios greater than 20, but $\varepsilon^{13}C$ (CO_2–C_1) values generally consistent with thermodynamic equilibrium. We speculate that, in these fields, methane was introduced to the basin but has had sufficient time and/or exposure to catalysts to approach C isotopic equilibrium with CO_2.

The relationship between methane and the higher order *n*-alkanes is further illuminated by the observation that 88% of measured hydrogen isotope fractionations between methane and higher-order hydrocarbons are consistent with thermodynamic equilibrium at their corresponding methane clumped isotope apparent temperature (*SI Appendix*, Fig. S6). However, only 30% of these gas samples are in carbon isotope equilibrium between methane and C_2 to C_5 species at that same temperature (Fig. 4). Specifically, gas samples with a low methane clumped isotope apparent temperature (0 °C to 120 °C) tend to have carbon isotope fractionations between methane and C_2 to C_5 alkanes that are greater than equilibrium at that methane apparent temperature and near the predicted compositions of products of homolytic cleavage or beta-scission, whereas samples with higher methane clumped isotope apparent temperatures tend to lie closer to the equilibrium fractionation line (Fig. 4*C*). Additionally, samples with low methane clumped isotope apparent temperatures tend to have lower methane $\delta^{13}C$ values, in the range commonly associated with biogenic gas, whereas samples with higher methane temperatures have higher methane $\delta^{13}C$ values, consistent with common ranges for thermogenic gas. These patterns of variation can be explained if the carbon isotope composition of thermogenic methane begins in or near equilibrium with coexisting C_2 to C_5 hydrocarbons when it first forms, but then subsequent addition of biogenic methane without subsequent participation in "metastable equilibrium" reactions involving the C_2 to C_5 hydrocarbons, lowers the $\delta^{13}C$ of methane, increasing values of $\varepsilon^{13}C$ (C_x-C_1) value (where x = 2 to 5). In the case of biogenic addition of methane, hydrogen isotope exchange among all hydrocarbons must keep pace with addition of this exotic methane, and the newly formed methane must generally be capable of exchanging carbon with coexisting CO_2, as these quasi-equilibria are maintained (Fig. 3 and *SI Appendix*, Figs. S2 and S6). Hydrogen exchange in *n*-alkanes has previously been documented to occur within approximately year timescales (34). So, in effect, only the methane carbon pool appears to remain

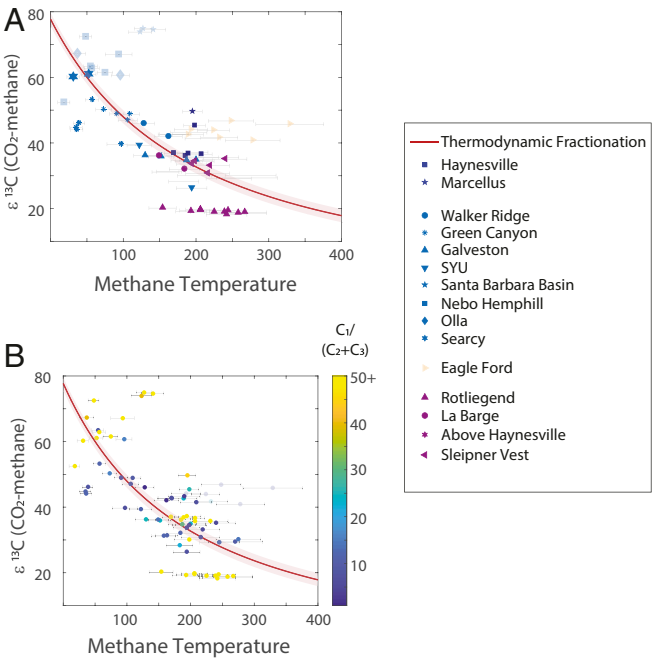

Fig. 3. $\varepsilon^{13}C$ (CO_2–methane) of carbon isotopes vs. methane temperature for gases in the study subdivided by (*A*) basin name and (*B*) gas wetness. Seventy-three percent of samples having $C_1/(C_2+C_3)$ values of less than 20 (excluding Eagleford) are consistent with the thermodynamic equilibrium fractionation (red solid line). Gases associated with biodegradation are shaded. The Eagle Ford gases are also shaded, as they are suspected to be influenced by a KIE in clumped isotopes of methane (26). The measurement errors for carbon isotopes of CO_2 and CH_4 are 0.5‰, and errors plotted for methane temperatures are 1σ.

isolated from the carbon pool in the C_2 to C_5 species once an exotic, low-$\delta^{13}C$ methane source has been introduced.

We also reexamined previously published isotopic data measured on products of pyrolysis experiments (both catalyzed and not) to see whether those systems also provide evidence for equilibrium processes (35–39). We confirm the previous suggestion that catalyzed pyrolysis generates gas components that approach equilibrium (35) (*SI Appendix*, Fig. S7); moreover, we find that noncatalyzed pyrolysis, despite producing gases with molecular proportions that differ from natural gases, also commonly exhibit intermolecular C and H isotope fractionations that approach equilibrium and differ from expectations for homolytic cleavage and beta-scission (*SI Appendix*, Fig. S8). This agreement is relatively close for lower-temperature noncatalyzed pyrolysis experiments (≤400 °C). Large departures from equilibrium are observed at the highest temperatures, generally falling to progressively larger intermolecular fractionations at higher temperatures—a pattern that contrasts with natural gases (*SI Appendix*, Fig. S9), equilibrium predictions, and models of well-defined kinetically controlled processes.

In summary, we find evidence that the distribution of stable isotopes among the C_1 to C_5 hydrocarbons and CO_2 in natural gas generally conform to two families of mutual quasi-equilibria: one being the C isotope contents of the C_2 to C_5 species plus the H isotope contents of all C_1 to C_5 species, and the second being C isotopes in methane and CO_2. Moreover, equilibrium intermolecular isotopic distributions are also observed in catalyzed pyrolysis experiments and noncatalyzed pyrolysis experiments conducted at relatively low temperatures (≤400 °C).

Radical Reaction Network Model. Most of the compounds present in natural gas (alkanes, aromatics, thiols, etc.) are thermodynamically metastable for the temperatures and pressures where they exist (16, 40). We explore whether our findings could reflect the attainment of a "metastable cyclic equilibrium," through a network of radical chain reactions among the gas species, dominated by fast radical transfer reaction and beta-scission leading to metastable equilibrium as has been previously suggested (28). We tested the plausibility of this hypothesis by constructing a model that tracks the distribution of ^{13}C among coexisting hydrocarbons that participate in free radical chain reactions. We do not address H isotope exchange in the model, as hydrogen in hydrocarbon molecules is more susceptible to isotope exchange than carbon under conditions seen in natural gas fields on timescales of days (34). Therefore, the equilibrium signature that we see in hydrogen isotope fractionation can be explained by an intermolecular hydrogen isotope equilibration, without implying a significant revision to common understanding of cracking reactions. Our carbon isotope model includes 24 species and 79 reactions, including initiation, H transfer, radical decomposition, radical termination, and radical addition reactions. We acquired kinetic parameters (activation energy and preexponential factor) for each reaction from the literature (41–43). We find that, when a ^{13}C spike is introduced in any of the species present at the outset of the model (methane, ethane, propane, and butane), that spike is transferred to all of the other hydrocarbon species, and, once steady state is reached, the $^{13}C/^{12}C$ ratio of each species equals the equilibrium value. This finding is true regardless of which species contains the ^{13}C spike when the model is initiated (*SI Appendix*, Fig. S10). At 500 K, our model comes to equilibrium within a year. We are unable to run the model at 423 K, due to limitations in computational power. However, in our model, the exchange rate is

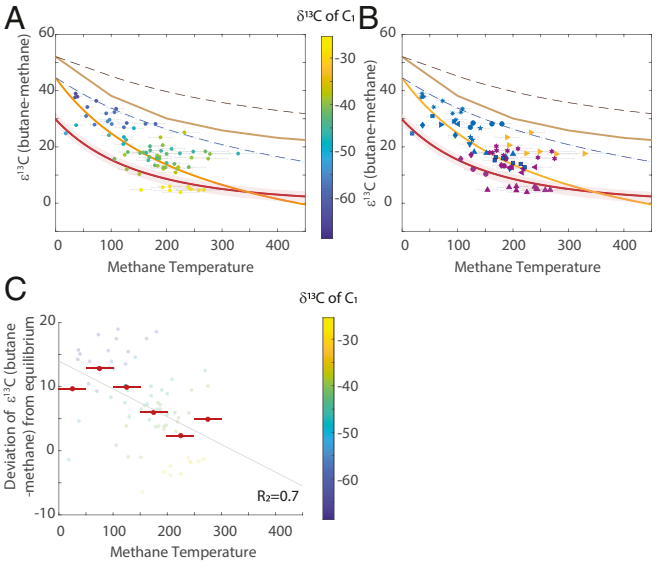

Fig. 4. $\varepsilon^{13}C$ (butane–methane) vs. methane clumped isotope apparent temperature for gases considered in this study color-coded by the corresponding $\delta^{13}C$ of methane for each (*A*) gas or (*B*) reservoir. Gas samples with low methane clumped isotope apparent temperatures also have low $\delta^{13}C$ of methane and tend to lie above the equilibrium line in this figure, near the curves for homolytic cleavage or β-scission, whereas gases with higher methane apparent temperatures have higher $\delta^{13}C$ of methane values and lie closer to the equilibrium fractionation line. This correlation is depicted in *C* and is consistent with an input of biogenic methane with very low $\delta^{13}C$ values at low methane temperatures, although we cannot rule out a contribution of low $\delta^{13}C$ values via kinetic processes. The red circles in *C* indicate binned averages over 50 °C intervals. We excluded the Eagle Ford gases for this calculation, as they are known to have a KIE affecting the methane temperatures. (See Fig. 2 for legend.) The measurement errors for carbon isotopes of butane and CH_4 are 0.5‰, and errors plotted for methane temperatures are 1σ.

limited by the radical initiation steps that have activation energies ranging from 51 kcal/mol to 88 kcal/mol (41). If we apply an Arrhenius relationship, the rate of those reactions decreases by a factor of 10^4 to 10^7 when the temperature changes from 500 K to 423 K. Therefore, we expect that the timescale of equilibration at geological temperatures will range from 10 kya to 10 Mya. Given these timescales, these reactions are geologically plausible and relevant. We propose that, similarly to our radical reaction model network, natural gas components exchange carbon with one another through multiple radical reactions, allowing their ^{13}C contents to approach equilibrium with one another.

Model for Natural Gas Formation. The preceding discussion and model of metastable cyclic equilibrium attempts to explain the pattern of equilibrium isotopic fractionations seen in C_2 to C_5 components of natural gases; but the exceptions to that pattern are equally significant (see *SI Appendix* for additional discussion on clumped isotopologues of small *n*-alkanes). We propose that three separate processes are responsible for the isotopic variations observed in natural gas components, and that the isotopic "fingerprint" of any one gas source reflects the unique combination of these processes.

First, we argue that the H isotope compositions of C_1 to C_5 hydrocarbons and C isotope compositions of C_2 to C_5 hydrocarbons often reflect an approach to metastable cyclic equilibrium during gas generation and/or deep subsurface storage. It has been previously argued that such metastable equilibrium requires catalysts to occur (27), although our reaction network model achieved the same end state over geologically relevant temperatures and times. We conclude that a metastable cyclic equilibrium might be aided by solid catalysts, but they are not required. An important point to note here is that the hydrocarbons in low-maturity systems are not generated in equilibrium, as seen in the two least-mature reservoirs in our dataset (Keathley Canyon and Walker Ridge), which fall near the β-scission fractionations and not near thermodynamic equilibrium. As maturity increases, the hydrocarbons fall closer to the equilibrium fractionation line. The approach to equilibrium is seen in moderate-maturity gases such as Santa Ynez Unit (SYU) and Green Canyon, while the attainment of equilibrium is seen in our most mature gases such as Hogsback, Above Haynesville, Sleipner Vest, and Galveston (Fig. 5).

Second, because we find that the CO_2–CH_4 pair generally attains carbon isotope equilibrium without either species necessarily being in C isotope equilibrium with C_{2+} hydrocarbons, we suggest that oxidation of methane to form CO_2 and reduction of CO_2 to form methane provides a second, effectively separate reaction network that allows these two species to maintain equilibrium without efficient C exchange with other species (18). This is reasonable because CH_4 is the slowest species to react in our model of hydrocarbon metastable cyclic equilibrium chemistry, for example, its hydrogen abstraction reactions being an order of magnitude slower than for other hydrocarbons (the k of reaction 78 listed in *SI Appendix* is one order of magnitude slower than reactions 53, 47, and 49). Therefore, it is easy to imagine cases where methane will react more quickly with oxidants than with hydrocarbon radicals. Additionally, C–C bonds in C_{2+} species are weaker and relatively easy to cleave compared to C–H or C–O bonds in CH_4 and CO_2. It is noteworthy that the CO_2–CH_4 system often approaches equilibrium at temperatures lower than established thermogenic gas generation temperatures and similar to reservoir conditions. For this reason, we suspect gases often enter shallow reservoirs near metastable cyclic equilibrium with respect to isotopic distributions among all molecular species, but, while gas is stored at shallower depths, methane oxidation and CO_2 reduction quickly redistribute ^{13}C between these two species. This redistribution could be driven by biological cycling of carbon between methanogens and methanotrophs, or it could reflect a catalyzed abiotic reaction (18).

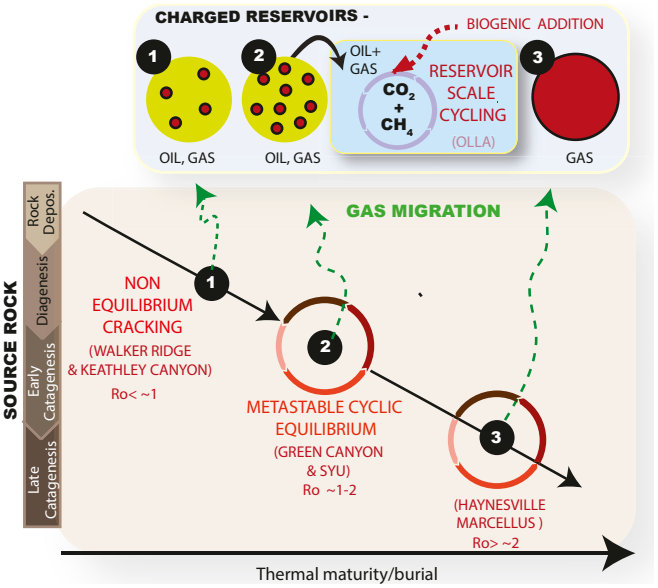

Fig. 5. Our model for *n*-alkane generation in natural gas reservoirs. Hydrocarbon species are initially produced by cracking mechanisms. This cracking signature is seen in very immature reservoirs such as Walker Ridge and Keathley Canyon. As maturity increases, the hydrocarbons fall closer to the equilibrium fractionation line. The approach to equilibrium is seen in moderate-maturity gases such as SYU and Green Canyon, while the attainment of equilibrium is seen in our most-mature gases such as Above Haynesville, Hogsback, Sleipner Vest, and Galveston. Ro indicates vitrinite reflectance, while green in the charged reservoirs indicates oil and red indicates gas.

Third, we see that the most marked departures from quasi-equilibrium isotope distributions among gas components, including highly aberrant C isotope fractionations among the C_{2+} species and/or between methane and C_{2+} species, are associated with recognized signatures of biodegraded gas (especially low ^{13}C of methane). This feature is seen in reservoirs such as Olla and Nebo Hemphill. We suggest that this signature becomes dominant when biogenic production of CH_4 and destruction of C_{2+} hydrocarbons has altered a large fraction of the initial gas charge, overwhelming the earlier signature of metastable cyclic equilibrium and sometimes outstripping the process that promotes quasi-equilibrium of C isotopes between CO_2 and CH_4.

The mechanisms we propose for hydrocarbon equilibration or CO_2–CH_4 equilibration are similar to previous suggestions that *n*-alkanes (and other small organic molecules) are in a metastable equilibrium with water in hydrocarbon reservoirs (16, 40). However, Helgeson et al. (16) suggested C_1-C_4 hydrocarbons, in particular, would not participate in these equilibrating reaction networks at the conditions of natural gas sources or reservoirs. This conclusion was largely a consequence of his estimates of reservoir $[O_2]$ concentrations. Our finding that these species commonly participate in metastable equilibrium with respect to C isotope distributions would be consistent with Helgeson et al.'s treatment of metastable equilibria if log fO_2(g) in hydrocarbon source rocks were ~0.5 lower than Helgeson et al. calculated.

Implications. Our primary finding, that natural gas formation generally occurs via reaction networks that incorporate metastable equilibrium between some subsets of species, has significant implications for central questions regarding the origins and fates of geological hydrocarbons: Where and when do natural gases form? What are the chemical proportions of major natural gas components, and how do they vary in time and space? These

questions are generally approached by merging models of basin thermal evolution with kinetic models for hydrocarbon generation that are based on extrapolations to geological conditions of the rates of gas and oil production in high-temperature, laboratory-timescale experiments. This method may still be the appropriate approach to predicting the onset of petroleum formation (i.e., as we find the least-mature natural gases express kinetically controlled fractionations), but, as petroleum systems deepen and thermally mature, the spatial and temporal distributions and chemical compositions of gases will be more strongly controlled by the relative thermodynamic stabilities of major components and their possible breakdown products; that is, high abundances of components may be buffered indefinitely where temperature, pressure, and fugacities of reactive species (e.g., O_2 and H_2) permit their persistence and destroyed where other compounds become more energetically favorable. Helgeson et al. (16) suggested that proportions of liquid, gas, and solid in petroleum-forming systems should be evaluated in a way analogous to how we use thermodynamic analysis of other quasi-equilibrium processes, such as partial fusion of rocks. The findings here extend this argument, suggesting that the partial pressures of gases of moderately to highly mature systems also follow thermodynamic principles. For example, one practical implication of this line of reasoning is that the conversion of "wet" (C_{2+}-rich) to "dry" (methane-dominated) gas is controlled by thermodynamic conditions (e.g., T, fO_2, and fH_2) and not only source rock maturity as it is conventionally understood. As such, any effort to predict the possible range in the abundance of economically and environmentally important volatile hydrocarbons should incorporate thermodynamic models alongside the thermal history of the source and reservoir interval in which they are generated and stored.

Methods

Methane Analysis. Methane (CH_4) was purified from mixed-gas samples using previously described methods (44). δD, $\delta^{13}C$, and Δ_{18} of methane were measured using the Ultra, using previously described methods (44), and reported in Dataset S1. δD and $\delta^{13}C$ values are expressed as $\delta D = ((R^2H_{sa}/R^2H_{VSMOW}) - 1)*1{,}000$, and $\delta^{13}C = ((R^{13}C_{sa}/R^{13}C_{VPDB}) - 1)*1{,}000$, where $R^2H = [D/H]$, $R^{13}C = [^{13}C/^{12}C)]$, VSMOW is Vienna Standard Mean Ocean Water, and VPDB is Vienna Pee Dee Belemnite. Clumped isotope compositions are expressed using Δ_{18} notation, where $\Delta_{18} = ((^{18}R/^{18}R^*) - 1)*1{,}000$, $^{18}R = [^{13}CH_3D] + [^{12}CH_2D_2]/[^{12}CH_4]$, and $18R^* = (6*[R^2H]^2) + (4*R^2H*R^{13}C)$; 18R* is the 18R value expected for a random internal distribution of isotopologues given the $\delta^{13}C$ and δD value of the sample (11). The specified isotope ratios are measured from the corresponding ion beam current ratios, standardized by comparison with a standard of known composition. Δ_{18} data are reported as per mil (‰), where 0‰ refers to a random distribution of methane isotopologues. We present measurement uncertainties for individual samples as 1 SE of the internal measurement variability for a single measurement. Reported uncertainties for inferred temperatures are propagated from the 1σ errors for Δ_{18} values. Finally, Δ_{18} values can be related to formation temperature (K) via the equation $\Delta_{18} = -0.0117*(10^6/T^2) + 0.708*(10^6/T^2) - 0.337$ (25).

Higher *n*-alkane Stable Isotope Measurements. Compositional analysis of gas samples was perfomed using gas chromatography (GC) as well as thermal conductivity and flame ionization detectors in Isotech Laboratories in Champaign, Illinois. Stable isotope values for gas components are measured using isotope ratio mass spectrometers and reported in Dataset S2. The gas samples are separated into individual components using a GC system. A cupric oxide furnace then combusts each component into CO_2 and H_2O. After purification, CO_2 is analyzed directly, whereas the H_2O is reacted with zinc to generate H_2 gas. We use error bars of 0.5‰ for carbon isotopes and 13‰ for hydrogen isotopes for all measured hydrocarbons (45).

All of the data reported in this manuscript are available in the *SI Appendix*.

1. A. R. Brandt *et al*., Energy and environment. Methane leaks from North American natural gas systems. *Science* **343**, 733–735 (2014).
2. J. F. Gent *et al*., Association of low-level ozone and fine particles with respiratory symptoms in children with asthma. *JAMA* **290**, 1859–1867 (2003).
3. M. E. Jenkin, K. C. Clemitshaw, Ozone and other secondary photochemical pollutants: Chemical processes governing their formation in the planetary boundary layer. *Atmos. Environ.* **34**, 2499–2527 (2000).
4. M. Schoell, The hydrogen and carbon isotopic composition of methane from natural gases of various origins. *Geochim. Cosmochim. Acta* **44**, 649–661 (1980).
5. B. P. Tissot, D. T. Welte, *Petroleum Formation and Occurence* (Springer Verlag, 1984).
6. J. M. Hunt, *Petroleum Geochemistry and Geology* (Freeman, 1995).
7. J. G. McNab, P. V. Smith, R. I. Betts, The evolution of petroleum. *Pet. Eng. Chem.* **44**, 2556–2563 (1952).
8. K. J. Jackśon, A. K. Burnham, R. L. Braun, K. G. Knauss, Temperature and pressure dependence of n-hexadecane cracking. *Org. Geochem.* **23**, 941–953 (1995).
9. R. J. Evans, G. T. Felbeck, High temperature simulation of petroleum formation I. The pyrolysis of Green River Shale. *Org. Geochem.* **4**, 135–144 (1983).
10. M. D. Lewan, M. J. Kotarba, D. Wieclaw, A. Piestrzynski, Evaluating transition-metal catalysis in gas generation from the Permian Kupferschiefer by hydrous pyrolysis. *Geochim. Cosmochim. Acta* **72**, 4069–4093 (2008).
11. L. C. Price, Thermal stability of hydrocarbons in nature: Limits, evidence, characteristics, and possible controls. *Geochim. Cosmochim. Acta* **57**, 3261–3280 (1993).
12. R. I. McNeil, W. O. BeMent, Thermal stability of hydrocarbons: Laboratory criteria and field examples. *Energy Fuels* **10**, 60–67 (1996).
13. L. C. Price, M. Schoell, Constraints on the origins of hydrocarbon gas from compositions of gases at their site of origin. *Nature* **378**, 368–371 (1995).
14. A. Prinzhofer, M. R. Mello, T. Takaki, Geochemical characterization of natural gas: A physical multivariable approach and its applications in maturity and migration estimates. *AAPG Bull.* **84**, 1152–1172 (2000).
15. D. A. Stolper *et al*., Distinguishing and understanding thermogenic and biogenic sources of methane using multiply substituted isotopologues. *Geochim. Cosmochim. Acta* **161**, 219–247 (2015).
16. H. C. Helgeson, A. M. Knox, C. E. Owens, E. I. Shock, Petroleum oil field waters, and authigenic mineral assemblages: Are they in metastable equilibrium in hydrocarbon reservoirs. *Geochim. Cosmochim. Acta* **57**, 3295–3339 (1993).
17. J. S. Seewald, Aqueous geochemistry of low molecular weight hydrocarbons at elevated temperatures and pressures: Constraints from mineral buffered laboratory experiments. *Geochim. Cosmochim. Acta* **65**, 1641–1664 (2001).
18. J. Horita, Carbon isotope exchange in the system CO_2-CH_4 at elevated temperatures. *Geochim. Cosmochim. Acta* **65**, 1907–1919 (2001).
19. Y. A. Taran, W. F. Giggenbach, "Geochemistry of light hydrocarbons in subduction-related volcanic and hydrothermal fluids" in *Volcanic, Geothermal, and Ore-Forming Fluids: Rulers and Witnesses of Processes within the Earth*, S. F. Simmons, I. Graham, Eds. (Society of Economic Geologists, 2005), pp. 61–74.
20. F. D. Mango, D. Jarvie, E. Herriman, Natural gas at thermodynamic equilibrium. Implications for the origin of natural gas. *Geochem. Trans.* **10**, 6 (2009).
21. F. D. Mango, D. M. Jarvie, Low-temperature gas from marine shales: Wet gas to dry gas over experimental time. *Geochem. Trans.* **10**, 10 (2009).
22. F. D. Mango, Transition metal catalysis in the generation of petroleum and natural gas. *Geochim. Cosmochim. Acta* **56**, 553–555 (1992).
23. F. D. Mango, J. W. Hightower, A. T. James, Role of transition-metal catalysis in the formation of natural gas. *Nature* **368**, 536–538 (1994).
24. D. A. Stolper *et al*., The utility of methane clumped isotopes to constrain the origins of methane in natural-gas accumulations. *Geol. Soc. Lond. Spec. Publ.* **468**, 23–52 (2018).
25. D. A. Stolper *et al*., Gas formation. Formation temperatures of thermogenic and biogenic methane. *Science* **344**, 1500–1503 (2014).
26. P. M. J. Douglas *et al*., Methane clumped isotopes: Progress and potential for a new isotopic tracer. *Org. Geochem.* **113**, 262–282 (2017).
27. Y. Ni, *et al*., Fundamental studies on kinetic isotope effect (KIE) of hydrogen isotope fractionation in natural gas systems. *Geochim. Cosmochim. Acta* **75**, 2696–2707 (2011).
28. Y. Xiao, Modeling the kinetics and mechanisms of petroleum and natural gas generation: A first principles approach. *Rev. Mineral. Geochem.* **42**, 383–436 (2001).
29. O. Sherwood, S. Scwietzke, V. Arling, G. Etiope, Global inventory of gas geochemistry data from fossil fuel, microbial and burning sources, version 2017. *Earth Syst. Sci. Data* **9**, 639–656 (2017).
30. A. M. Martini, J. M. Budai, L. M. Walter, M. Schoell, Microbial generation of economic accumulations of methane within a shallow organic-rich shale. *Nature* **383**, 155–158 (1996).
31. A. M. Martini *et al*., Microbial production and modification of gases in sedimentary basins: A geochemical case study from a Devonian shale gas play, Michigan basin. *AAPG Bull.* **87**, 1355–1375 (2003).
32. J. S. Seewald, Organic-inorganic interactions in petroleum-producing sedimentary basins. *Nature* **426**, 327–333 (2003).
33. W. J. Stahl, Carbon and nitrogen isotopes in hydrocarbon research and exploration. *Chem. Geol.* **20**, 121–149 (1977).
34. E. P. Reeves, J. S. Seewald, S. P. Sylva, Hydrogen isotope exchange between *n*-alkanes and water under hydrothermal conditions. *Geochim. Cosmochim. Acta* **77**, 582–599 (2012).
35. F. D. Mango, L. W. Elrod, The carbon isotopic composition of catalytic gas: A comparative analysis with natural gas. *Geochim. Cosmochim. Acta* **63**, 1097–1106 (1999).
36. F. Lorant, A. Prinzhofer, F. Behar, A.-Y. Huc, Carbon isotopic and molecular constraints on the formation and the expulsion of thermogenic hydrocarbon gases. *Chem. Geol.* **147**, 249–264 (1998).
37. C. Pan, L. Jiang, J. Liu, S. Zhang, G. Zhu, The effects of calcite and montmorillonite on oil cracking in confined pyrolysis experiments. *Org. Geochem.* **41**, 611–626 (2010).

38. B. Andresen, T. Throndsen, A. Råheim, J. Bolstad, A comparison of pyrolysis products with models for natural gas generation. *Chem. Geol.* **126**, 261–280 (1995).
39. J. Du, Z. Jin, H. Xie, L. Bai, W. Liu, Stable carbon isotope compositions of gaseous hydrocarbons produced from high pressure and high temperature pyrolysis of lignite. *Org. Geochem.* **34**, 97–104 (2003).
40. J. S. Seewald, Evidence for metastable equilibrium between hydrocarbons under hydrothermal conditions. *Nature* **370**, 285–287 (1994).
41. K. M. Sundaram, G. F. Froment, Modeling of thermal cracking kinetics. 3. Radical mechanisms for the pyrolysis of simple paraffins, olefins, and their mixtures. *Ind. Eng. Chem. Fund.* **17**, 174–182 (1978).
42. J. R. Fincke *et al*., Plasma thermal conversion of methane to acetylene. *Plasma Chem. Plasma Process.* **22**, 105–136 (2002).
43. H. Wang, M. Frenklach, A detailed kinetic modeling study of aromatics formation in laminar premixed acetylene and ethylene flames. *Combust. Flame* **110**, 173–221 (1997).
44. D. A. Stolper *et al*., Combined ^{13}C–D and D–D clumping in methane: Methods and preliminary results. *Geochim. Cosmochim. Acta* **126**, 169–191 (2014).
45. T. Umezawa *et al*., Interlaboratory comparison of δ13C and δD measurements of atmospheric CH4 for combined use of data sets from different laboratories. *Atmos. Meas. Tech.* **11**, 1207–1231 (2018).
46. M. J. Whiticar, "Correlation of natural gases with their sources" in *The Petroleum System-From Source to Trap* , L. B. Magoon, W. G. Dow, Eds. (AAPG Special Volume, American Association of Petroleum Geologists, 1994), Vol. 60, pp. 261–283.